

# Characteristics of Recovery Motion Resulting From Side Contact With a Physical Assistant Robot Worn During Gait

Yasuhiro Akiyama , *Member, IEEE*, Ryota Kushida, Shogo Okamoto , *Member, IEEE*, and Yoji Yamada, *Member, IEEE*

**Abstract**—Although a wearable assist robot helps to enhance the gait ability of the wearer, it can cause gait instability in an emergency. A collision with an environmental object is one source of such instability. Insufficient adaptation to change by the physical frame, and restriction of joint motion, increases the risk of collision and fall of the wearer owing to the robot. In this article, the reaction motion owing to side contact, which applies a spin moment to the body, is investigated for the wearers of a physical assistant robot. In particular, reaction motions in the horizontal plane, such as body rotation, foot direction, and center-of-mass position, are investigated. Factor analysis and cluster analysis are performed, and two reaction patterns—the rotation group and the straight group—are determined. The motion of these groups suggests an approach for navigation through an obstacle while using an assist robot. Furthermore, the gait phase at collision time is considered as a determinant of the reaction pattern and the reaction pattern is found to affect the fall mode. The results of the article suggest that the joints of the physical assistant robot should be equipped with sufficient degrees of freedom, at least in hip rotation, such that it is capable of rotating the body and feet in the horizontal plane to reduce fall risk.

**Index Terms**—Collision, fall risk, gait motion, physical assistant robot, reaction motion.

## I. INTRODUCTION

RECENTLY, physical assistant robots have been utilized outside hospitals for improving labor productivity and the mobility of the elderly [1]. Many experimental and commercial robots have been developed to be used in society without any external physical support [2], [3]. Although some robots have balance control or have a supporting device, such as a cane [4], [5], most robots used for worker require the wearer to maintain balance themselves.

Manuscript received February 25, 2019; revised December 1, 2019 and April 8, 2020; accepted May 24, 2020. This article was recommended by Associate Editor K. Li. This work was supported by the Japan Society for the Promotion of Science KAKENHI under Grant 26750121. (*Corresponding author: Yasuhiro Akiyama.*)

The authors are with the Department of Mechanical Systems Engineering, Nagoya University, Nagoya 464-8601, Japan (e-mail: akiyama-yasuhiro@mech.nagoya-u.ac.jp; r\_kushida@icloud.com; okamoto-shogo@mech.nagoya-u.ac.jp; yamada-yoji@mech.nagoya-u.ac.jp).

This article has supplementary downloadable material available at <https://ieeexplore.ieee.org>, provided by the authors.

Color versions of one or more of the figures in this article are available online at <https://ieeexplore.ieee.org>.

Digital Object Identifier 10.1109/THMS.2020.3016098

However, falls, which are general accidents that occur during walking, can occur while using physical assistant robots and cause serious injury. Because such fall injuries consume significant social resources [6], [7], there is a need to decrease fall hazards.

An assist robot can reduce the risk of falls by improving the gait ability of the wearer. However, the robot can potentially cause motion instability and falls because of the mismatch of motion and the restriction of joint movements. Fukui *et al.* discovered that the limitation related to the degrees of freedom (DOF) of joints, which originates from the joint mechanism, changes gait motion during curving motions [8], [9]. Such restriction of motion limits recovery motion, which aims to avoid a fall in an emergency. Some assist robots, which do not have rigid joints, slightly restrict the motion of the wearer [10]. However, the rigid joint robot is necessary, especially in industrial usage, considering the robot's capacity to provide assist torque. The mismatch of assistive motion, which affects recovery motion acting against perturbations, should also be considered [11]. If the assistive torque distributes the motion of the wearer because of mismatch, the robot will increase the risk of a fall.

Furthermore, biomechanical studies suggest that the mass and inertia of the robot also affect the motion of the wearer [12], [13]. The physical frame expansion caused by attaching an assist robot can also become a source of tripping or collision with an environmental object. Such contact can easily occur in narrow environments, such as a room or the corridor of an apartment. The risk of falls caused by an assist robot is a critical issue for the safety of wearers and for the development of assist robots; therefore these risks must be analyzed and minimized.

The collision between the side of the robot and an obstacle is unique to an assist robot and needs to be considered. Many assist robots laterally expand the physical frame of the wearer. Side contact with the robot can generate spin moment to the wearer. To control and stop body spin, a lateral step and/or rotation of foot direction is necessary. However, the joint restriction caused by the assist robot may impede this reaction motion. Therefore, methods to reduce body imbalance caused by this unique perturbation should be considered. Previously, we observed the reaction motion against side contact and identified strategies for recovering motion. However, the observed parameters and analysis were limited to the direction of pelvis and insufficient to investigate the motion of lower limb [14].

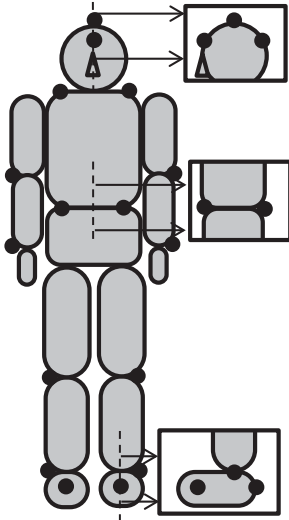


Fig. 1. Marker setting (anterior and posterior superior iliac spines, knees, and ankles were estimated using cluster markers).

In this article, the reaction motion owing to contact between a walking human wearing a physical assistant robot and environmental objects is investigated. In contrast to a general perturbation that may occur while walking, such as tripping and slipping, the contact of the robot side with an obstacle that applies a rotational moment in the horizontal plane of the wearer is considered. The reaction motions should differ from those—motions occurring in a sagittal plane—reported previously [15]–[17]. Thus, to identify and evaluate the risk of a fall caused by collision with an environmental object, the reaction motion owing to side contact is observed and analyzed in this study.

## II. METHOD

The experiment was performed with the permission of the institutional review board of Nagoya University.

### A. Apparatus

The experiment was carried out using a walking lane with dimensions of approximately  $5\text{ m} \times 8\text{ m}$ . The recording area was approximately  $4\text{ m} \times 5\text{ m}$ , wherein the acceleration and deceleration areas were excluded. The motion in the recording area was recorded using ten cameras of a three-dimensional motion capture system (MAC 3-D system, Motion Analysis Corporation, Rohnert Park, CA, USA) at 120 Hz. A set of critical markers of a SIMM Motion Module (SIMM, MulsculoGraphics Inc., Evanston, IL, USA) was attached (see Fig. 1). Cluster markers were used for positions where motion capture cameras could not directly detect motion owing to the interruption of the line of vision by the wearable robot or some other equipment. The cluster markers were used for anterior and posterior superior iliac spines, knees, and ankles. The ground reaction force (GRF) was recorded at 120 Hz using mobile six-axis force plates (M3D, Tec Gihan Co., Ltd., Kyoto, Japan) fixed under the soles of the participants.



Fig. 2. Assist robot (left: front view, right: back view).

A wearable robot named Motor Actuated Lower-Limb Orthosis (MALO) was used in this experiment (see Fig. 2). MALO is attached to the wearer using a pelvis corset, thigh and shank cuffs, and shoes. It weighs approximately 12 kg and is supported by the ground through a leg frame. MALO's three joints—hip, knee, and ankle—have a single DOF and can rotate in the sagittal plane. The hip and knee joints are actuated by an electric motor (RE 40, Maxon Motor AG, Sachseln, Switzerland). The assist pattern was designed to help both stance and swing leg. At the stance phase, hip extension is assisted for 15%–45% of the gait cycle (GC). Furthermore, knee flexion torque is applied for 30–60% GC. These assists were designed to help move the trunk forward. Moreover, assistive torque, which helps to expand the step length, is applied during the swing phase. It consists of hip flexion torque between 65% GC and 95% GC and knee extension torque between 75% GC and 95% GC. An assistive torque of 7 N·m, which starts and ends smoothly, was applied to each joint and phase. The magnitude and timing of the assist were set by reference values used to assist devices and biomechanics [10], [18], [19].

An aluminum frame obstacle was fixed on the sides of the walking lane to hit the side of MALO. The contact area of the obstacle was a metal plate, whose contact force in the axis normal to the contact surface was measured using a force sensor (Dyn Pick, Wacoh-Tech Inc., Tokyo, Japan). The height of the contact plate was made adjustable to allow contact with the upper and lower sides of the upper thigh of MALO. The position of the obstacle in the lateral and frontal directions was also adjustable to control the contact phase and position.

Subjects wore goggles, with covered lower halves, to prevent anticipation of the obstacle. To stabilize the gait motion and timing, an electric metronome and a speed guide, which was driven by an electric motor, were used. Protectors were attached to the knees, elbows, and hands of the subject for safety. A body harness, hung from a gondola and placed on the rail over the walking lane, was used to support the subject before ground contact when a fall occurred. The gondola was pulled using an electric motor to follow the walking subject. A schematic providing an overview of the experimental setup is shown in Fig. 3.

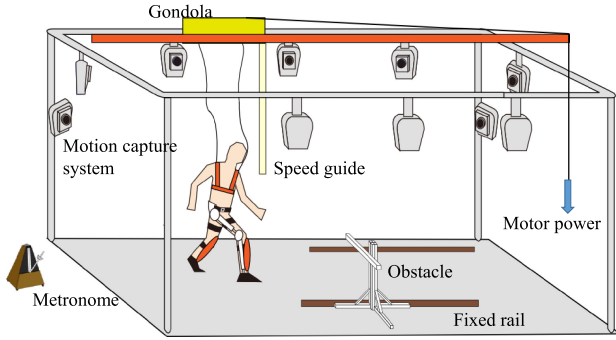


Fig. 3. Experimental setup.

### B. Subjects

Eight healthy male subjects participated in the experiment as simulated workers using the assist robots. The average age of participants was 21.9 years old, with a standard deviation (SD) of 2.0. Their mean height and weight were 169.8 cm ( $\pm 4.7$  SD) and 60.1 kg ( $\pm 4.7$  SD), respectively. Previous studies have suggested that despite a decrease in the motion speed and response time decrease caused by aging, the strategy of fall avoidance motion is the same for young adults and the elderly [20]–[22]. Thus, we opine that the results of this study will be applicable, to some extent, to the elderly.

### C. Protocol

After an informed consent procedure, the subjects wore well-fitted sportswear, protectors, a body harness, and MALO, whose size was adjusted to fit each subject. Next, reflective markers for the motion capture system were attached. To adapt to MALO, the subject walked the lane repeatedly until their gait motion stabilized. The speed and cadence of the recorded trial were set to match the gait timing observed in this training session. The recording of trials, then, began.

During the experiment, the subject repeatedly walked straight down the lane. Occasionally, the lateral side of MALO collided into an obstacle fixed beside the walking lane. The position and height of the obstacle were adjusted to achieve different contact conditions. Two levels of height (upper and lower sides of the thigh) were set to evaluate the effect of the contact region as different contact regions affected the force and moment applied to the subject. The effects of the tripping phase on the reaction motion have been previously reported [15], [23], especially those between early and late swing phases. Therefore, the contact phase was also considered a parameter that affected the reaction motion. Because the range of motion of the contact region on the thigh—the affected part in the trip experiment—in the traveling direction was less than a foot during a swing phase, it was difficult to make repeatable and stable contact at a specific phase. To observe the reaction motion under various contact phases, the position of the obstacle was set at two different locations. Each location made contact at the early swing and late swing phases, based on the relative position of the stance foot and the obstacle in the walking direction, at the time of contact. The early swing condition locates the stance foot forward to the obstacle at the

time of contact. The late swing condition identifies the reverse position. The accurate gait phase at the time of contact was calculated posteriori.

The combination of conditions, which consisted of two contact parts and two obstacle positions, was repeated four times. Therefore, 16 contact trials were tested for each subject. To prevent anticipation of the contact condition, the order of conditions was randomized and 24 dummy trials, in which no contact occurred, were inserted. Furthermore, half of the contacts occurred on the opposite side to prevent anticipation. Thus, a total of 40 trials were conducted for each subject.

### D. Data Processing

The recorded motion was smoothed using a 6-Hz Butterworth filter. The gait event time, which includes heel contact (HC) and toe-off (TO), was detected on the basis of GRF, with a threshold of 10 N. The speed was calculated by dividing the trace of the head marker in the traveling direction by the motion duration in each trial. The cadence was calculated as the inverse of the time difference between HCs of both legs. Step length was determined as the distance between the heel markers of successive steps in the traveling direction. The step width was calculated by using the same method as that for step length, except for the direction, which was orthogonal to the traveling direction. The position of the center of mass (CoM) of the whole body was calculated by using Zatsiorsky’s method [24]. The gait phase was calculated as the percentage of the GC, which is the time and distance traveled between successive HCs of the leading leg. The contact phase was defined as the ratio of the time between the contact time (CT) and the last HC of the swing leg in relation to the duration of the average GC. Because the duration of the GC changes slightly, the contact phase includes some error.

Generally, a reaction motion occurring soon after a gait perturbation is critical to avoid a fall and determines the amount of freedom for successive motion [20], [25]. Thus, four motion events were defined during the reaction motion. The CT is defined as the time of contact with the obstacle. Because the subject lowered the leg after contact, the HC of the affected leg (AHC) is defined as the time when the affected leg touches the floor. The subject then starts to swing the opposite leg. The TO of the recovery leg (RTO) is defined as the time when the recovery leg separates from the floor. The HC of the recovery leg (RHC) is the time when the recovery leg touches the floor. The CT was detected by using the video recording. The other events were detected using force plates attached under the sole, as mentioned in Section II-A.

To analyze the reaction motion against the side contact, physical parameters that represent the motion through the time of contact to the recovery step were selected. Abbreviations and definitions of each parameter are given in Table I. The parameters listed in Table I are separated by relation to the contact condition, GRF, and reaction motion. A coordinate system of parameters was determined in global coordinates. The traveling direction of the walking lane was defined as the “forward” direction and the “lateral” direction was defined as the direction orthogonal to the traveling direction. The “normal” direction was identical to

TABLE I  
PARAMETERS OF CONTACT AND REACTION MOTION

Category	Name	Definition
Parameters of contact state	$IF_{peak}$	Maximum impact force in forward direction [N]
	$IF_{impulse}$	Impulse in forward direction [N·s]
	$IT_{hit}$	Gait phase at the contact timing [%GC]
	$IS_{hit}$	Speed of CoM in forward direction at the contact timing [m/s]
	$D\text{CoM}_f, D\text{CoM}_l, D\text{CoM}$	Distance between obstacle and CoM at CT in forward, lateral, and horizontal directions [m]
	$D\text{Leg}_f, D\text{Leg}_l, D\text{Leg}$	Distance between obstacle and stance leg at CT in forward and lateral directions [m]
Parameters of ground reaction force	$GRI_f\text{-Aleg}, GRI_l\text{-Aleg}, GRI_n\text{-Aleg}$	Impulse of affected leg between AHC to RHC in forward, lateral, and normal directions [N·s]
	$GRM\text{-Aleg}$	Integral of moment around normal axis of affected leg between AHC to RHC [N·m·s]
	$GRI_f\text{-Rleg}, GRI_l\text{-Rleg}, GRI_n\text{-Rleg}$	Impulse of recovery leg between CT to RTO in forward, lateral, and normal directions [N·s]
	$GRM\text{-Rleg}$	Integral of moment around normal axis of recovery leg between CT to RTO [N·m·s]
Parameters of reaction motion	$PEL_{ang}\text{-RTO}$ and $PEL_{vel}\text{-RTO}$	Pelvis rotation angle and angle velocity at RTO [deg, deg/s]
	$PEL_{ang}\text{-RHC}$ and $PEL_{vel}\text{-RHC}$	Pelvis rotation angle and angle velocity at RHC [deg, deg/s]
	$ST_l$ and $ST_w$	Step length and width of recovery step [m]
	$F_{ang}\text{-Rleg}$ and $F_{ang}\text{-Aleg}$	Rotation angle of recovery and affected leg at RHC [deg]

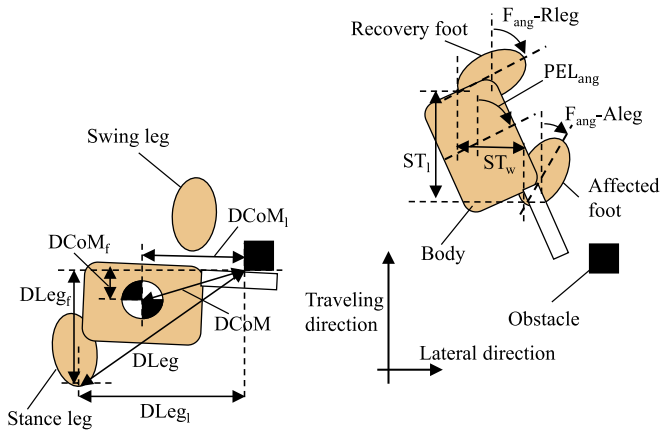


Fig. 4. Definition of posture parameters (left: CT, right: RHC).

the vertical direction. The rotation toward the object was set as a positive yaw angle, which became zero when the pelvis and foot were placed in the forward direction. The definitions of CT and RHC parameters are shown in Fig. 4.

The correlation of these parameters was calculated to check for relationships. Factor analysis was used to identify representative strategies of reaction motion and extract the characteristics of each strategy. In the field of gait analysis, Lord *et al.* [26] identified a factor that determines the difference in gait motion between young and older adults. Various human motions, such as straight gait, about-face turn, sit-to-stand motion, and others, were analyzed by Chong [27]. Akiyama *et al.* [28] also used factor analysis to extract the characteristics of the natural

curving motion of humans. After the  $z$ -scores of the parameters were determined, the MATLAB “factoran” function, which uses the maximum likelihood estimation and Bartlett’s method, was applied to the parameters. Major factors were then rotated using the varimax method.

Factors that represent the characteristics of reaction motion against side contact were then used for cluster analysis. Cluster analysis, based on Ward’s method [29], was used to separate trials into groups in which trials exerted the same reaction strategy and had a similar parameter value trend. The feature of each group identified the mechanism of each reaction strategy. The differences in the physical parameters across groups were statistically tested. First, the parameters were compared across groups by using multivariate analysis of variance (MANOVA) [30]. Then, each parameter was compared by using the  $t$ -test [31].

A total of 320 trials, which included 128 contact trials, were conducted for eight subjects. From these trials, approximately ten trials were extracted from dummy trials from each subject to determine the normal gait. The gait time for a normal GC was calculated as the average value of these trials. Among all of the contact trials, only 77 were analyzed in Section III because the others, which included critical marker hiding, failure of contact, and unique reaction, did not fit into the framework of this study.

Failure of contact includes contact at a double stance phase, contact of unintended parts of the robot or subject, and weak contact. In contrast, the unique reaction motion, which includes holding out and a strategy based on “elevating” [15], was not a failure of contact. Although the “elevating” strategy was an effective reaction against side contact, it was only frequently observed for particular subjects in our experiment. Because these

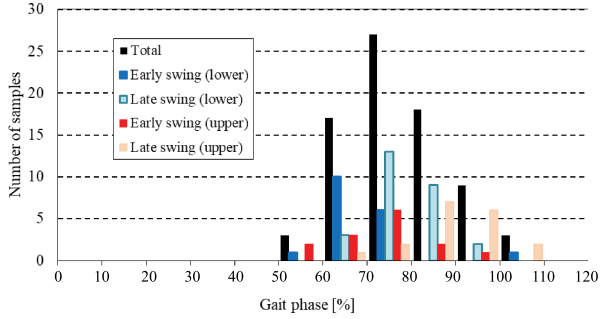


Fig. 5. Distribution of CT aggregated with each 10% of the GC. The number of trials is 77 in total. They are distributed to each condition as 18, 27, 14, and 18, respectively.

unique reaction motions were not commonly observed and could not fit into the framework of this article, such motions were excluded from the analysis. It should be mentioned that there were no reaction motions, such as backward movement, that were more hazardous than those previously described herein.

Recorded reaction motions of contact trials were combined across subjects in the analysis process. In this article, the effect of the difference of the contact side was ignored. All contact trials were considered the contact of the right side by symmetrically transforming the motion and force of the left side contact trials against the vertical plane parallel to the walking lane.

### III. RESULTS

#### A. Gait Parameters

The parameter of normal gait motion was calculated from dummy trials. The mean values of the gait parameters of each subject were distributed in the ranges 3.71–4.77 km/h (walking speed), 47.3–61.1 strides/min (cadence), and 56.8–81.5 cm (step length). The speed, cadence, and step length were slightly smaller than those previously reported [32], [33].

The distribution of the contact phase is shown in Fig. 5. Although the number of trials with 70%–80% GC contact phase is the largest, the contact phase was broadly distributed in the swing phase. Ideally, the contact phase is the time period between the HC and contact divided by the time period between successive HCs. However, the gait motion was disturbed by the contact. Therefore, it is impossible to obtain the time of HC soon after the contact, such that the gait motion is not disturbed. The contact phase was, thus, estimated as the time period between HC and contact divided by the average GC of dummy trials. As a result of this approximation, the contact phase includes some error owing to variability of gait motion in each trial. Although the contact phases of the three trials exceeded 100% (with contact phases of 101.0%, 102.3%, and 105.0%), the contact of these trials occurred in the swing phase. The same number of trials was conducted for each condition, the contact position and phase, but the number of analyzed trials differed among conditions as follows: 18 early swing phases with lower part contact; 27 late swing phases with lower part contact; 14 early swing phases with upper part contact; and 18 late swing phases with upper part contact. Furthermore, as shown in Fig. 5, the contact of the

lower part condition tended to occur in an earlier phase of the GC than that of the upper part condition.

The correlation matrix of parameters, which represent the contact condition and reaction motion, is shown in Table II.

#### B. Factor Analysis

To extract the characteristics of reaction motion, factor analysis was applied using parameters selected from Table II that reflect the reaction motion and force.

Four major factors, which explain 66.5% of the sample variance, were extracted. The breakdown of contributions of first, second, third, and fourth factors was 22.8%, 16.8%, 14.2%, and 12.7%, respectively. They were calculated as the percentage of the total variance of each factor. The number of factors was determined by considering the contribution and describability combination of the loading of each factor. The loadings of each factor, after being scaled by the contribution ratios, are shown in Fig. 6.

1) *First Factor (Rotation Factor)*: The rotation factor represents the body rotation that occurs because of the rotation moment applied by side contact. According to Fig. 6, large positive factor loadings appear in  $PEL_{vel-RTO}$ ,  $PEL_{ang-RHC}$ , and  $PEL_{vel-RHC}$ . These parameters represent the amount of rotational motion of the body in the horizontal plane during the recovery swing. Furthermore,  $F_{ang-Rleg}$  and  $F_{ang-Aleg}$  are also large and positive. These parameters represent the change of direction of the feet after contact. Overall, the first factor is strongly related to the pelvis rotation in the clockwise direction during the recovery motion.

2) *Second Factor (Straight Factor)*: This factor represents motion toward the traveling direction. The loading of the second factor became large and positive in  $ST_1$ , which is the length of the recovery step. A large step length, which is the result of a long forward motion of the recovery leg, means that the subject moved in the forward direction. Large positive  $GRI_f-Aleg$  and  $GRM-Aleg$  values also represent the same motion trend.  $GRI_f-Aleg$  and  $GRM-Aleg$  suggest that the subject thrust his body forward and rotated in the counterclockwise direction. However, it should be noted that a large positive  $PEL_{ang-RTO}$  is not consistent with this trend.

3) *Third Factor*: This factor is related to the GRF and ground reaction torque of the recovery leg. The factor loadings of  $GRI_1-Rleg$  were positive and  $GRM-Rleg$  was negative. In addition,  $GRI_n-Rleg$  was positive. It seems that the motion represented by this factor is one that is approaching the obstacle and, therefore, risks additional contact.

4) *Fourth Factor*: This factor is also related to the GRF and torque. The positive  $GRI_f-Aleg$  and  $GRM-Aleg$  are related to the straight motion of the second factor. Furthermore, a large negative  $GRI_1-Aleg$ , which is the motion that separates the test subject from the obstacle, and positive  $GRI_f-Rleg$ , which is the push-off force of the recovery step, strengthen straight motion.

#### C. Classification of Reaction Motion in Factor Space

Among the four major factors, the first and second factors were selected for cluster analysis. These factors denote

TABLE II  
CORRELATION COEFFICIENTS AMONG PARAMETERS

	Parameters of contact state										Parameters of ground reaction force										Parameters of reaction motion									
	IF <sub>peak</sub>	IF <sub>impulse</sub>	IT <sub>hit</sub>	IS <sub>hit</sub>	DCom <sub>f</sub>	DCom <sub>i</sub>	DCoM	DLeg <sub>r</sub>	DLeg <sub>i</sub>	DLeg	GRI <sub>f</sub> -Aleg	GRI <sub>f</sub> -Rleg	GRM <sub>f</sub> -Aleg	GRM <sub>f</sub> -Rleg	GRI <sub>f</sub> -Aleg	GRI <sub>f</sub> -Rleg	GRM <sub>f</sub> -Aleg	GRM <sub>f</sub> -Rleg	PEL <sub>ang</sub> -RHC	PEL <sub>ang</sub> -RTO	PEL <sub>ang</sub> -RHC	PEL <sub>ang</sub> -RTO	ST <sub>w</sub>	ST <sub>l</sub>	F <sub>ang</sub> -Rleg	F <sub>ang</sub> -Aleg				
IF <sub>peak</sub>	0.76																													
IF <sub>impulse</sub>		0.76																												
IT <sub>hit</sub>			0.13																											
IS <sub>hit</sub>				0.13																										
DCom <sub>f</sub>					0.13																									
DCom <sub>i</sub>						0.76																								
DCoM							0.76																							
DLeg <sub>r</sub>								0.89																						
DLeg <sub>i</sub>									0.89																					
DLeg										0.26																				
GRI <sub>f</sub> -Aleg											0.13																			
GRI <sub>f</sub> -Rleg												0.13																		
GRM <sub>f</sub> -Aleg													0.07																	
GRM <sub>f</sub> -Rleg														0.07																
PEL <sub>ang</sub> -RTO															0.24															
PEL <sub>ang</sub> -RHC																0.18														
PEL <sub>ang</sub> -RTO																	0.26													
PEL <sub>ang</sub> -RHC																		0.26												
PEL <sub>ang</sub> -RHC																			0.18											
PEL <sub>ang</sub> -RTO																				0.16										
PEL <sub>ang</sub> -RHC																					0.36									
PEL <sub>ang</sub> -RTO																						0.32								
PEL <sub>ang</sub> -RHC																							0.20							
PEL <sub>ang</sub> -RTO																								0.20						
PEL <sub>ang</sub> -RHC																									0.20					
PEL <sub>ang</sub> -RTO																										0.20				
PEL <sub>ang</sub> -RHC																											0.20			
ST <sub>w</sub>																											0.16			
ST <sub>l</sub>																											0.01			
F <sub>ang</sub> -Rleg																											0.33			
F <sub>ang</sub> -Aleg																											0.25			

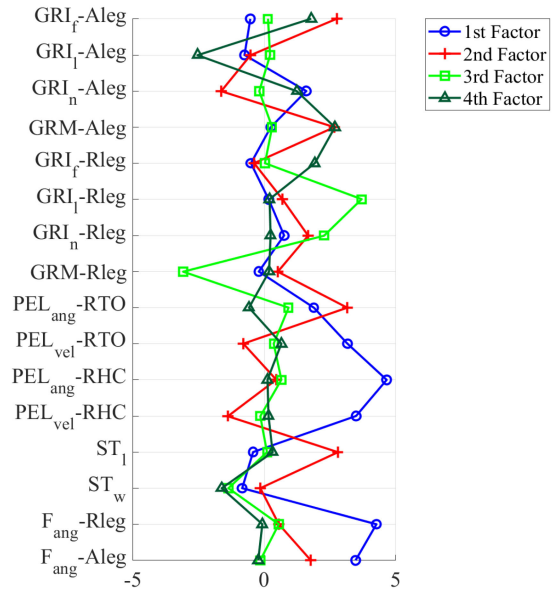


Fig. 6. Factor loading. The contribution of each factor is 22.8%, 16.8%, 14.2%, and 12.7%.

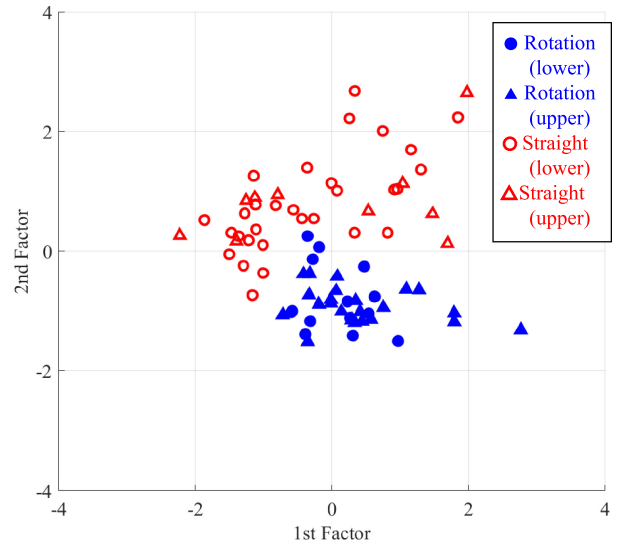


Fig. 7. Distribution of factor score of each trial.

representative aspects of the reaction motion. The first factor represents the rotation motion of the body in the clockwise direction, which reflects the moment exerted by the contact. On the other hand, the second factor represents the strength of the motion, which advances the body forward.

As a result of the cluster analysis, two groups with different reaction motions were identified. The distribution of trials is displayed in Fig. 7. Each group corresponds to the factor score of the first and second factors. Most trials of the group denoted as the “rotation group” had a positive score for the first factor and a negative score for the second factor. The other group, which was denoted as the “straight group,” tended to have a positive second factor.

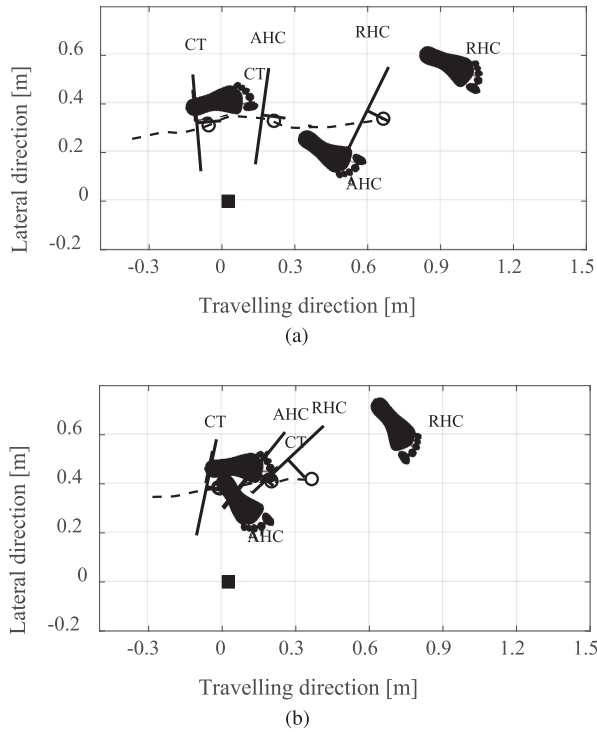


Fig. 8. Footprint of each group at representative timings (Square: obstacle, Circle: center of gravity of the subject, Convex bar: position and direction of pelvis). (a) Straight group. (b) Rotation group.

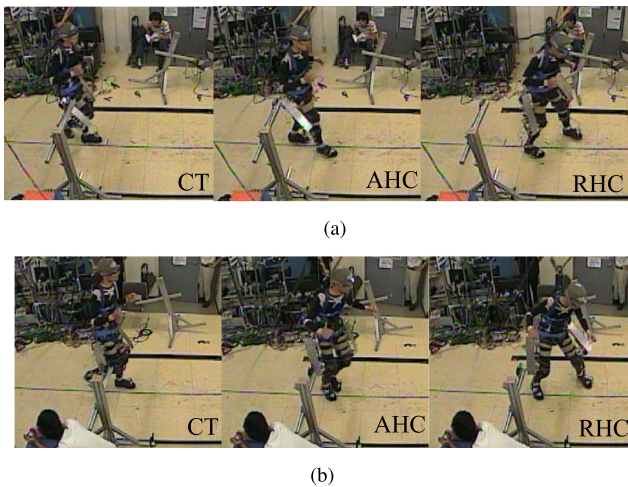


Fig. 9. Snapshot of each group at representative timings. (a) Straight group. (b) Rotation group.

From the 77 trials, which consisted of 45 lower position contacts and 32 upper position contacts, 37 trials were classified as the rotation group (15 lower positions and 22 upper positions). Thus, the straight group consisted of 40 trials (30 lower position contacts and 10 upper position contacts).

Footprint images in lateral and traveling directions, and snapshots that represent typical motions of each group, are displayed in Figs. 8 and 9, respectively. The posture, GRF, and assist profile collected after tripping are displayed in Fig. 10. The position and direction of the footprints represent the characteristics of

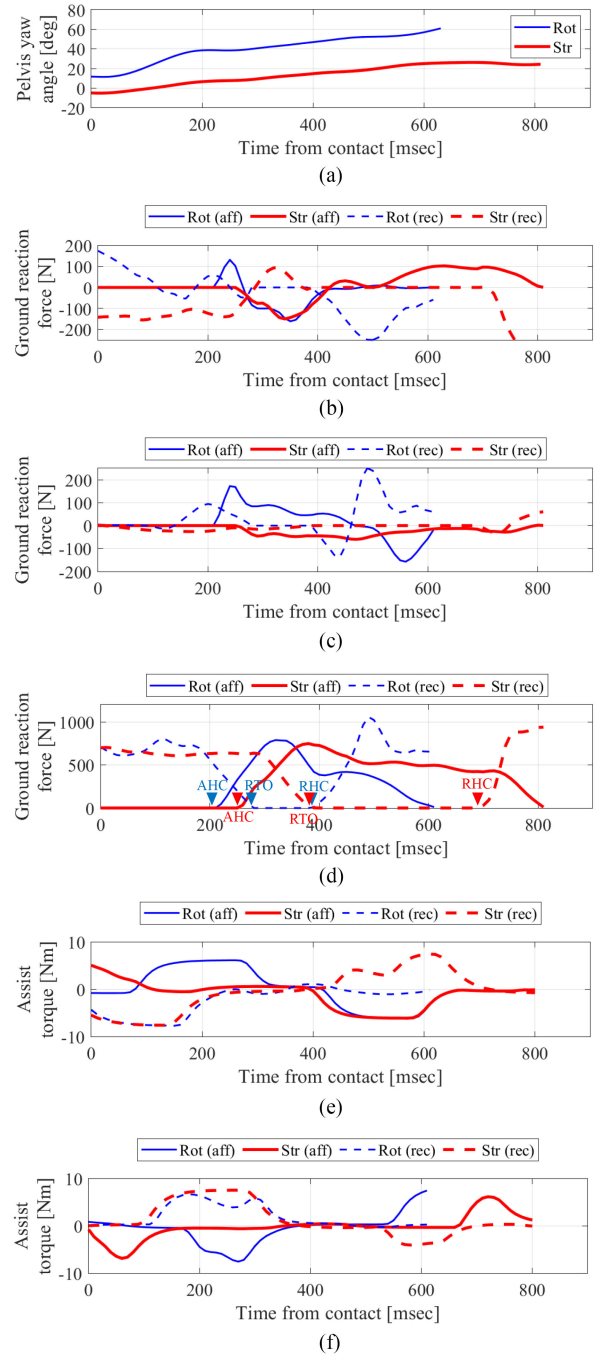


Fig. 10. Motion after tripping (the horizontal axis begins from CT) (Str = straight, Rot = rotation). (a) Pelvis angle. (b) GRF (forward direction). (c) GRF (lateral direction). (d) GRF (vertical direction). (e) Assist torque (hip). (f) Assist torque (knee).

the reaction motion of each group. For the case of the rotation group, the step length toward the traveling direction shortened and the direction of the footprint changed toward the affected side. In contrast, the footprint of the straight group moved forward and was directed toward the traveling direction, even after tripping. The footprint suggested that, in the rotation group, the subject interrupted the straight walk and concentrated more on avoiding the obstacle. However, in the straight group, the

subject passed the side of the obstacle without decelerating or drastically changing the gait motion.

#### D. Difference of Parameters Between Rotation and Straight Groups

The MANOVA results show that the set of parameters for each group differed significantly ( $p < 0.01$ ). Thus, to inspect the characteristics of each group in detail, the parameters listed in Table II were compared by using the  $t$ -test.

1) *Parameters Strongly Related to the Classification*: Because the first and second factors were used for classification, parameters that strongly relate to these factors represent each group. As mentioned above, rotation of pelvis, direction of foot, length of recovery step, and GRF of the affected leg were considered as the parameters. According to Fig. 11, which compares these parameters across groups, these factors were consistent with the characteristics of each group.

2) *Parameters Used in the Factor Analysis*: Residual parameters of reaction motion and force used in the factor analysis, although the contribution was low, are shown in Fig. 12. However, these residual parameters do not differ significantly across groups, except for GRI-Rleg.

3) *Parameters Related to Contact State*: Parameters related to the contact state were not used in the factor analysis to analyze the characteristics of reaction motion. However, it should be considered that the contact condition affects the reaction motion. Therefore, the parameters of the contact state of each group were compared. Fig. 13 shows that the gait phase at the CT, the relative position of the CoM, and the obstacle at the AHC differ significantly, whereas the difference between the contact force and impulse was not significant.

## IV. DISCUSSION

### A. Characteristics of Reaction Motions

1) *Rotational Group*: The parameters of the first factor, such as pelvis rotation and foot angle, suggest that the reaction motion of this group is represented by body rotation. The rapid increase in  $PEL_{ang}$  during the recovery step represents this rotational motion. Although it seems that this reaction motion attempts to stop body rotation and go through the obstacle, the body rotation does not stop, even at the RHC. According to the reaction motion shown in Fig. 9, hip abduction and outer rotation occurred, whereas the hip joint did not have the DOF in those directions. This is because the subject's inner torque exceeded the rigidity of the hip joint of the assistive robot.

2) *Straight Group*: The parameters that configured the second factor, such as step length, GRF, and torque of the affected leg, suggest that the reaction motion of this group is represented by a continuous gait in the traveling direction. The long step length directly represents the characteristics of this motion. The thrust force and counterclockwise movement of the affected leg support this motion. Although the motion was less than that of the rotation group, the hip joint also rotated outside the direction of flexion/extension.

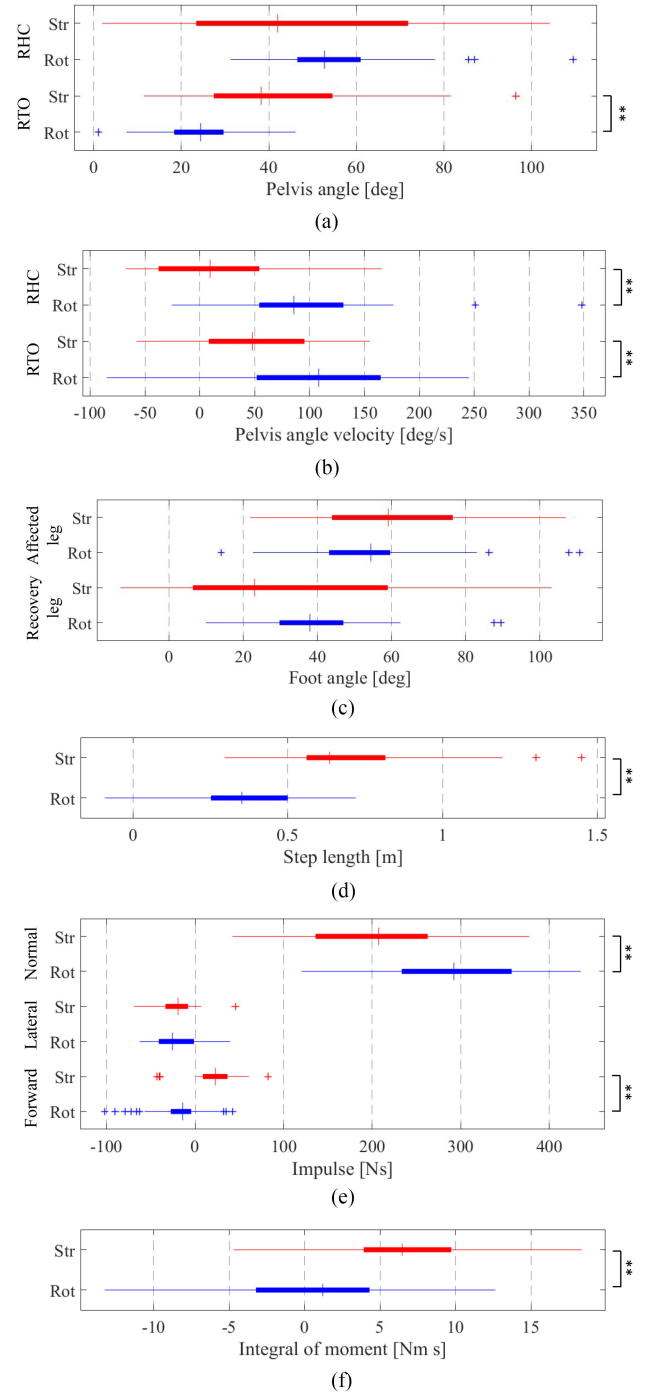


Fig. 11. Major parameters of first and second factor (maximum whisker length:  $1.5 \times$  interquartile range,  $p$ -value:  $+ < 0.1$ ,  $* < 0.05$ ,  $** < 0.01$ ) (Str = straight, Rot = rotation). (a) Pelvis angle ( $PEL_{ang}$ ). (b) Pelvis angle velocity ( $PEL_{vel}$ ). (c) Foot direction ( $F_{ang}$ ). (d) Step length ( $ST_1$ ). (e) GRF of affected leg (GRI-Aleg). (f) Ground reaction moment of affected leg (GRM-Aleg).

### B. Parameter That Affects the Selection of Reaction Motion

The contact condition, which includes contact position, force, and posture, is likely to have affected the reaction motion. However, Fig. 13(a) and (b) suggests that the impact force and impulse did not significantly differ among the trials for different groups. Furthermore, the moment arm of body rotation, which

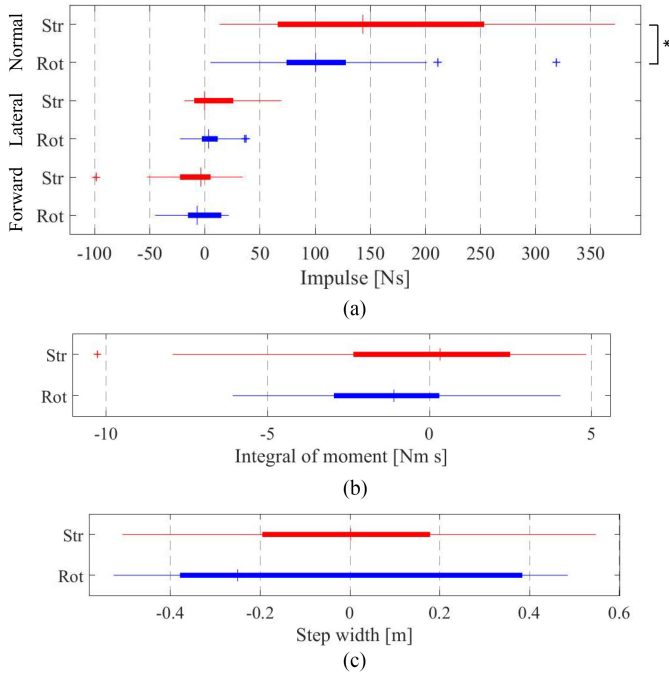


Fig. 12. Minor parameters of first and second factor (maximum whisker length:  $1.5 \times$  interquartile range,  $p$ -value:  $+<0.1$ ,  $*<0.05$ ,  $**<0.01$ ) (Str = straight, Rot = rotation). (a) GRF of recovery leg (GRI-Rleg). (b) Ground reaction moment of recovery leg (GRM-Rleg). (c) Step width ( $ST_w$ ).

may be the distance between the obstacle and body in the lateral direction, did not differ significantly, as shown in Fig. 13(e) and (f). This result is different from a simple inspection, which shows that the large rotation moment caused the body rotation.

The distance between the obstacle and the stance leg was longer in the rotation group, as shown in Fig. 13(f). Furthermore, according to Fig. 13(c), the gait phase at the CT significantly differed across groups. It should also be noted that the position of the contact is different across groups, as shown in Fig. 7. As shown in Fig. 5, the contact position and phase were strongly related in this experiment. Therefore, it can be said that the rotation motion frequently occurred at the upper position and late in the swing contact, whereas the straight motion occurred at the lower position and early in the swing contact. The contact position likely came closer to the stance leg early in the swing contact because the swing leg passed below the trunk in this phase, whereas the contact position on the swing leg moved forward in the late swing phase. Thus, at the time of late contact, the posture and motion of the body became more unbalanced. It seems that the contact phase, which corresponds to each body posture, affected the reaction motion more than the contact position in this experiment. However, because it is difficult to analyze the effect of contact position and phase independently (a limitation of experimental conditions), another series of experiments is required to analyze this point in detail.

According to Fig. 13(d), the contact speed differed across groups. However, the contact speed could also be related to the contact phase. According to Table II, contact speed is strongly correlated to the contact phase, as well as the distance between the obstacle and the stance leg. Thus, it is also difficult to

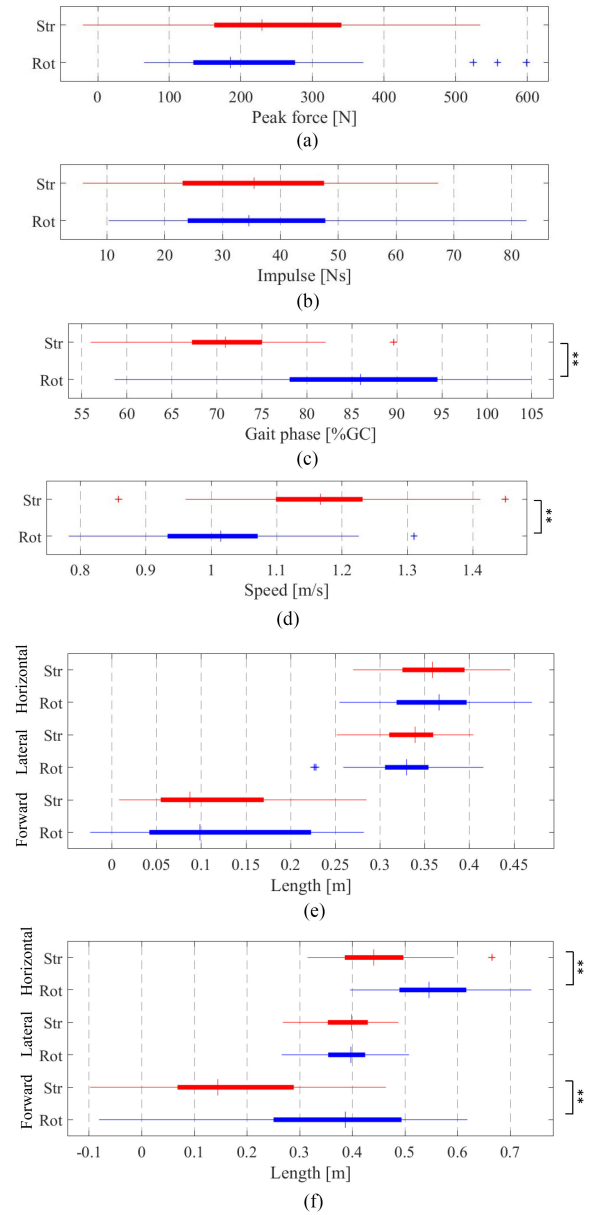


Fig. 13. Parameters of contact state (maximum whisker length:  $1.5 \times$  interquartile range,  $p$ -value:  $+<0.1$ ,  $*<0.05$ ,  $**<0.01$ ). (a) Peak interaction force ( $IF_{peak}$ ). (b) Impulse of interaction force ( $IF_{impulse}$ ). (c) Gait phase of contact timing ( $IT_{hit}$ ). (d) Contact speed ( $IS_{hit}$ ). (e) Distance between obstacle and CoM (DCoM). (f) Distance between obstacle and stance leg (DLeg).

investigate the effect of contact speed independently from the effect of contact phase and position. However, physically, the higher speed probably enhances to exert the straight motion because the subject with a large inertial force is likely to continue stepping forward. This is another point that can be considered in a future study.

### C. Measures to Reduce the Risk of Fall

The rotation group is characterized by large body rotation. Thus, it is anticipated that falls occur when the body rotation cannot be stopped and body imbalance increases. For example,

the failure of the rotation reaction occurs when the joint restriction disturbs the recovery step in the lateral direction. A fall from the lateral or back position, which is easily caused by a rotation fall, can result in severe injuries, such as a bone fracture of the hip or pelvis [34].

In contrast, the reaction motion of the straight group indicated that motion mainly occurs in the sagittal plane. The recovery leg placed forward controls the forward moment of the body. The failure of moment reduction, which is caused by a slower and shorter recovery step and insufficient GRF and moment, leads to a forward fall. A forward fall can result in an arm fracture and face or head injuries [35], [36].

An effective countermeasure against fall injuries should be considered for each reaction group because of their different fall modes. For rotation group falls, implementation of additional joint DOF, such as hip rotation and adduction/abduction to the assist robot, is one method for increasing the performance of recovery motion as joint restriction disturbs the reaction motion of the wearer [8], [9]. In addition, implementation of protectors to the lateral or back side of the hip is an effective solution for mitigating fall injuries [37], [38]. A protective measure applied to the upper limbs can be effective [35], [39] in the case of the straight group. Furthermore, improvement of the assist algorithm can contribute to a decrease in the risk of falls by accelerating, or not preventing the swing of the recovery leg, and enforcing the support of the recovery leg. While the evaluation of the effect of the assist algorithm was not a focus of this study, it is important to evaluate its performance against fall arrest motion in future studies.

#### D. Limitation of This Study

This study is the investigation of the effect of spin moment applied by the side contact of the robot on the reaction motion. For the parameters of contact condition, we selected contact part, which was upper or lower thigh, and the timing, which was early or late swing phase. However, there could be other parameters that probably affect the reaction motion. For example, the assist algorithm, mass and shape of the robot, and the rigidity of the fixation part probably affect the selection and performance of the reaction motion. Furthermore, the variation in gait timing such as speed, cadence, and step length should be considered in future analysis.

#### V. CONCLUSION

Reaction motions used to avoid falls caused by the unintended contact of a physical assistant robot with an obstacle were observed and analyzed in this article. Contact with the side of the robot was investigated while considering the probability and severity of anticipated hazards and the physical assistant robot's contribution to safety. Factor analysis and cluster analysis were used to extract the characteristics of the reaction motion recorded in the experiment.

As a result, it was discovered that the subjects' reaction motion against some contact can be classified into two groups: the rotation group and the straight group. The subjects rotated their bodies in the horizontal plane to control the yaw moment caused

by contact in the case of the rotation group. In the case of the straight group, subjects stopped their forward body rotation in the sagittal plane using appropriate positioning and loading of the recovery leg. These reaction motions may have appeared owing to differences in body postures; however, body posture was not analyzed separately from the contact position.

The difference of the motion of these recovery strategies suggests that the mode of falls, injuries, and countermeasures differed across the strategies adopted. Furthermore, the motion of the rotation group required a step in the lateral direction, wherein the joint DOF is restricted by most assist robots. The results of this study suggest that the implementation of additional joint DOF would contribute to an increase in fall avoidance motions and, therefore, mitigate fall injuries.

#### REFERENCES

- [1] S. Mohammed, Y. Amirat, and H. Rifai, "Lower-limb movement assistance through wearable robots: State of the art and challenges," *Adv. Robot.*, vol. 26, no. 1/2, pp. 1–22, 2012.
- [2] B. Chen *et al.*, "Recent developments and challenges of lower extremity exoskeletons," *J. Orthopaedic Transl.*, vol. 5, pp. 26–37, 2016.
- [3] S. Viteckova, P. Kutilek, and M. Jirina, "Wearable lower limb robotics: A review," *Biocybern. Biomed. Eng.*, vol. 33, no. 2, pp. 96–105, 2013.
- [4] P. J. Manns, C. Hurd, and J. F. Yang, "Perspectives of people with spinal cord injury learning to walk using a powered exoskeleton," *J. Neuroeng. Rehabil.*, vol. 16, no. 1, 2019, Art. no. 94.
- [5] C. Tefertiller *et al.*, "Initial outcomes from a multicenter study utilizing the Indego powered exoskeleton in spinal cord injury," *Topics Spinal Cord Injury Rehabil.*, vol. 24, no. 1, pp. 78–85, 2017.
- [6] D. G. Tate, "Workers' disability and return to work," *Amer. J. Phys. Med. Rehabil.*, vol. 71, no. 2, pp. 92–96, 1992.
- [7] H. J. Lipscomb, J. E. Glazner, J. Bondy, K. Guarini, and D. Lezotte, "Injuries from slips and trips in construction," *Appl. Ergonom.*, vol. 37, no. 3, pp. 267–274, 2006.
- [8] Y. Fukui, Y. Akiyama, Y. Yamada, and S. Okamoto, "The change of gait motion when curving a corner owing to the motion restriction caused by a wearable device," in *Proc. IEEE Int. Conf. Syst., Man, Cybern.*, 2017, pp. 525–530.
- [9] E. Kramer, Y. Akiyama, Y. Fukui, and Y. Yamada, "The change of gait motion during curvilinear obstacle avoidance while restricted by a wearable robotic device," in *Proc. 7th IEEE Int. Conf. Biomed. Robot. Biomechatronics*, 2018, pp. 928–933.
- [10] A. T. Asbeck, S. M. De Rossi, K. G. Holt, and C. J. Walsh, "A biologically inspired soft exosuit for walking assistance," *Int. J. Robot. Res.*, vol. 34, no. 6, pp. 744–762, 2015.
- [11] Y. Akiyama, I. Higo, Y. Yamada, and S. Okamoto, "Analysis of recovery motion of human to prevent fall in response to abnormality with a physical assistant robot," in *Proc. IEEE Int. Conf. Robot. Biomimetics*, 2014, pp. 1493–1498.
- [12] E. Kodesh, M. Kafri, G. Dar, and R. Dickstein, "Walking speed, unilateral leg loading, and step symmetry in young adults," *Gait Posture*, vol. 35, no. 1, pp. 66–69, 2012.
- [13] J. Meuleman, W. Terpstra, E. H. van Asseldonk, and H. van der Kooij, "Effect of added inertia on the pelvis on gait," in *Proc. IEEE Int. Conf. Rehabil. Robot.*, 2011, pp. 1–6.
- [14] Y. Akiyama, R. Kushida, Y. Yamada, and S. Okamoto, "An analysis of recovery motion of a man wearing physical assistant robot in response to collision," in *Proc. IEEE Int. Conf. Syst., Man, Cybern.*, 2015, pp. 1089–1093.
- [15] J. J. Eng, D. A. Winter, and A. E. Patla, "Strategies for recovery from a trip in early and late swing during human walking," *Exp. Brain Res.*, vol. 102, no. 2, pp. 339–349, 1994.
- [16] M. Temel, K. S. Rudolph, and S. K. Agrawal, "Gait recovery in healthy subjects: Perturbations to the knee motion with a smart knee brace," *Adv. Robot.*, vol. 25, no. 15, pp. 1857–1877, 2011.
- [17] T. M. Owings, M. J. Pavol, and M. D. Grabiner, "Mechanisms of failed recovery following postural perturbations on a motorized treadmill mimic those associated with an actual forward trip," *Clin. Biomechanics*, vol. 16, no. 9, pp. 813–819, 2001.

- [18] C. L. Lewis and D. P. Ferris, "Invariant hip moment pattern while walking with a robotic hip exoskeleton," *J. Biomechanics*, vol. 44, pp. 789–793, 2011.
- [19] K. Shamaei, M. Cenciari, A. A. Adams, K. N. Gregorczyk, J. M. Schiffman, and A. M. Dollar, "Design and evaluation of a quasi-passive knee exoskeleton for investigation of motor adaptation in lower extremity joints," *IEEE Trans. Biomed. Eng.*, vol. 61, no. 6, pp. 1809–1821, Jun. 2014.
- [20] M. J. Pavol, T. M. Owings, K. T. Foley, and M. D. Grabner, "Mechanisms leading to a fall from an induced trip in healthy older adults," *J. Gerontol. Ser. A, Biol. Sci. Med. Sci.*, vol. 56, no. 7, pp. M428–M437, 2001.
- [21] M. Pijnappels, M. F. Bobbert, and J. H. van Dieën, "Push-off reactions in recovery after tripping discriminate young subjects, older non-fallers and older fallers," *Gait Posture*, vol. 21, no. 4, pp. 388–394, 2005.
- [22] D. G. Thelen, L. A. Wojcik, A. B. Schultz, J. A. Ashton-Miller, and N. B. Alexander, "Age differences in using a rapid step to regain balance during a forward fall," *J. Gerontol. Ser. A, Biol. Sci. Med. Sci.*, vol. 52, no. 1, pp. M8–M13, 1997.
- [23] V. Dietz, J. Quintern, G. Boos, and W. Berger, "Obstruction of the swing phase during gait: Phase-dependent bilateral leg muscle coordination," *Brain Res.*, vol. 384, no. 1, pp. 166–169, 1986.
- [24] P. De Leva, "Adjustments to Zatsiorsky-Seluyanov's segment inertia parameters," *J. Biomechanics*, vol. 29, no. 9, pp. 1223–1230, 1996.
- [25] H. Nagano, P. Levinger, C. Downie, A. Hayes, and R. Begg, "Contribution of lower limb eccentric work and different step responses to balance recovery among older adults," *Gait Posture*, vol. 42, no. 3, pp. 257–262, 2015.
- [26] S. Lord, B. Galna, J. Verghese, S. Coleman, D. Burn, and L. Rochester, "Independent domains of gait in older adults and associated motor and nonmotor attributes: Validation of a factor analysis approach," *J. Gerontol. Ser. A, Biomed. Sci. Med. Sci.*, vol. 68, no. 7, pp. 820–827, 2012.
- [27] R. K. Chong, "Factor analysis of the functional limitations test in healthy individuals," *Gait Posture*, vol. 28, pp. 144–149, 2008.
- [28] Y. Akiyama, S. Okamoto, H. Toda, T. Ogura, and Y. Yamada, "Gait motion for naturally curving variously shaped corners," *Adv. Robot.*, vol. 32, no. 2, pp. 77–88, 2018.
- [29] J. H. Ward Jr., "Hierarchical grouping to optimize an objective function," *J. Amer. Statist. Assoc.*, vol. 58, no. 301, pp. 236–244, 1963.
- [30] R. G. O'Brien and M. K. Kaiser, "MANOVA method for analyzing repeated measures designs: An extensive primer," *Psychol. Bull.*, vol. 97, no. 2, pp. 316–333, 1985.
- [31] M. P. Fay and M. A. Proschan, "Wilcoxon-Mann-Whitney or t-test? On assumptions for hypothesis tests and multiple interpretations of decision rules," *Statist. Surv.*, vol. 4, pp. 1–39, 2010.
- [32] F. Finley and K. Cody, "Locomotive characteristics of urban pedestrians," *Arch. Phys. Med. Rehabil.*, vol. 51, no. 7, pp. 423–423, 1970.
- [33] D. J. Blanke and P. A. Hageman, "Comparison of gait of young men and elderly men," *Phys. Therapy*, vol. 69, no. 2, pp. 144–148, 1989.
- [34] R. A. Marottoli, L. F. Berkman, and L. M. Cooney Jr., "Decline in physical function following hip fracture," *J. Amer. Geriatrics Soc.*, vol. 40, no. 9, pp. 861–866, 1992.
- [35] K. DeGoede, J. Ashton-Miller, and A. Schultz, "Fall-related upper body injuries in the older adult: A review of the biomechanical issues," *J. Biomechanics*, vol. 36, no. 7, pp. 1043–1053, 2003.
- [36] K. M. DeGoede and J. A. Ashton-Miller, "Biomechanical simulations of forward fall arrests: Effects of upper extremity arrest strategy, gender and aging-related declines in muscle strength," *J. Biomechanics*, vol. 36, no. 3, pp. 413–420, 2003.
- [37] S. R. Cummings and M. C. Nevitt, "A hypothesis: The causes of hip fractures," *J. Gerontol.*, vol. 44, no. 5, pp. M107–M111, 1989.
- [38] A. Harada, M. Mizuno, M. Takemura, H. Tokuda, H. Okuizumi, and N. Niino, "Hip fracture prevention trial using hip protectors in Japanese nursing homes," *Osteoporosis Int.*, vol. 12, no. 3, pp. 215–221, 2001.
- [39] S. Abdolshah, Y. Akiyama, K. Mitsuoka, Y. Yamada, and S. Okamoto, "Analysis of upper extremity motion during trip-induced falls," in *Proc. 26th IEEE Int. Symp. Robot Human Interactive Commun.*, 2017, pp. 1485–1490.